

Prediction of Presence of Brain Tumor Utilizing Some State-of-the-Art Machine Learning Approaches

Mitrabinda Khuntia, Prabhat Kumar Sahu, Swagatika Devi

Dept. of Computer Science and Engineering, ITER, S'O'A University, Bhubaneswar, India

Abstract—A brain tumor is a kind of abnormal development caused by unregularized cell reproduction and it is increasing day-by-day. The Magnetic Resonance Imaging (MRI) tools are the most often used diagnostic tool for brain tumor detection. However, ample amount of information contained in MRI makes the detection and analysis process tedious and time consuming. The ability to accurately identify the exact size and proper location of a brain tumor is a tough task for radiologists. Medical image processing is an interdisciplinary discipline in which image processing is a tough research. Image segmentation is the prime requirement in image processing as it separates dubious regions from biomedical images thereby enhancing the treatment reliability. In this regard, our article reviews eight existing binary classifiers to compare their results for designing an automated Computer Aided Diagnosis (CAD) system. The proposed classification models can analyze T1-weighted brain MRI images to reach at a conclusion. The classification accuracy advocates the quality of our work.

Keywords—Brain tumor classification; MRI; SVM; decision tree; random forest; CAD

I. INTRODUCTION

The proper diagnosis of some crucial information is a key challenge in the field of bioinformatics or medical research. Many diagnostic and research institutions include a wealth of medical diagnosis data. It is barely essential to categorize them in order to automate and speed up illness diagnosis.

A continuous progression in cancer research has been carried out during the previous decades [1]. Scientists used a number of approaches, including very early-stage screening, to identify the disease before symptoms appeared. They have also developed noble methods for detecting the disease therapy results early on [16]. As a result of the advent of new medical technology, large amounts of cancer data have been gathered and made available to the clinical research community. Hence, medical researchers are exclusively employing popular machine learning techniques which can discover patterns and connections from massive datasets and anticipate future cancer outcomes with high accuracy.

The automated segmentation and categorization of medical images is crucial in brain tumor diagnosis, prognosis of tumor development, and therapy. Early diagnosis of a brain tumor predicts a faster response in therapy, which improves patient survival rates. Manual procedures used in normal clinical work to find and categorize brain tumors in large medical image collections incur considerable effort and time costs. It is desirable and beneficial to have a procedure for automatic detection, localization, and classification. Any disruption may intimate disease and injury. The identification of brain tumors is crucial in biological applications. Several procedures, like

as preprocessing, feature extraction, and classification, are required during the classification process.

Various medical imaging modalities are utilized to give tumor related information that is required for detection [2]. Prime methods include computed tomography (CT), single-photon emission computed tomography (SPECT), positron emission tomography (PET), magnetic resonance spectroscopy (MRS), and magnetic resonance imaging (MRI). MRI collection produces numerous 2D picture slices with strong tissue contrast while taking benefit of no ionising radiation [2]. T2 images are more suitable for identifying the borders of edoema areas. Brain tumors are identified and classified using MRI image processing.

II. LITERATURE SURVEY

Iftekharruddin et al.[5] used fractal wavelet characteristics as input to a Self Organizing Map (SOM) classifier and attained an average accuracy of 90%. Based on histogram study of temporal Magnetic Resonance Image (MRI) data, Manikis et al [14] developed a unique paradigm for monitoring tumor alterations. The proposed method detects tumor distribution and quantitatively predicts its development or decrease, possibly benefiting clinicians in objectively analysing tiny changes throughout therapy. Roy et al. [15] proposed an investigation towards automated brain tumor identification and classification using brain MRI. Brain tumor segmentation was a critical method for collecting information from complex MRI images of the brain. Sindhushree K.S et al [6] created and tested a strategy for segmenting brain tumors using two-dimensional MRI data. Discovered tumors are also shown in three dimensions. To identify malignancy, high pass filtering, histogram equalization, thresholding, morphological methods, along with segmentation employing linked component labeling were used. The recovered 2D tumor pictures were rebuilt into 3D volumetric data, and the tumor volume was determined.

Havaei et al.[6] designed a semi-automatic method using kNN classifier. They used the well-known BRATS 2013 dataset and done both whole and core tests, with Dice similarities of 0.85 for the total tumor region and 0.75 for the core tumor area. Sachdeva et al.[3] semi-automatically constructed the tumor contour and then calculated 71 features using the intensity profile, co-occurrence matrix, and Gabor functions. The classifiers Support Vector Machine (SVM) and Artificial Neural Network (ANN) were compared. Similarly, Kaur[4] presented autonomous brain tumor classification approach with ten features and a Back Propagation Neural Network as the classifier, which had a 95.3% accuracy.

Mohsen et al. [9] suggested a deep learning based classifier paired with discrete wavelet transform (DWT) and principal

components analysis to categorize a dataset including three distinct brain tumors (PCA). Four other deep learning-related research with equivalent goal employ the same dataset as we used in this study, which is crucial for comparing and evaluating the proposed model's performance outcomes. Pashaei et al. [11] suggested two approaches for classification: the first employed a CNN model for classification, while the second used CNN characteristics as inputs to a KELM methodology. The KELM algorithm is a learning algorithm composed of hidden node layers. A two-layer CNN design was introduced by Abiwinanda et al. [10]. A CNN with 16 convolution layers was proposed by Sultan et al. [12]. In another work, Anaraki et al. [13] introduced a hybrid approach for network design enhancement that combines the usage of CNNs with genetic algorithm (GA) criteria.

III. BRAIN TUMOR DIAGNOSIS

Brain is a centralized processing unit in humans that senses, controls, and runs all of our bodily functions. Neurons and Galilean cells are the two types of cells that make up the brain. Brain tumor refers to an unexpected proliferation of brain cells in the brain. Brain tumors can be either malignant or non-cancerous. The examination of tumors in the identification of malignant characteristics is a tough work owing to the variable nature of the tumor and its similarity to other regions of the brain. Early discovery of this impact has a higher possibility of recovery than late diagnosis. However, in today's world, the vast majority of tumors are identified at a late stage. As a result, early stage detection is a critical necessity.

IV. PROPOSED FRAMEWORK

A. Dataset Used

Benign cases are classed as positive in our study, whereas malignant ones are classified as negative as shown in Fig. 1 and fig. 2. Linear correlations are straight-line correlations between two variables with values ranging from -1 to + 1, where -1 represents the ideal negative relationship and + 1 represents the ideal positive relationship. By identifying the relationship between nine aspects of benign and malignant classes, the Pearson correlation between positive and negative classes is presented.

B. Block Diagram of the System

Before training the model, we collected images, partitioned the dataset, and investigated augmentation alternatives. The model is fine-tuned, and the outcomes were enhanced. The confusion matrix, model loss, and model accuracy have all been proven to show the loss and accuracy change with epoch. The proposed block diagram displays the whole classifier system in the simplest way possible as presented in Fig. 3. Decision making is a key component of this scheme and serves an important role in the research.

C. Data Preprocessing

Data preprocessing is used to fill in blanks, locate and eliminate outliers, and resolve self-contradiction. The sample code number has been removed from the dataset since it has no effect on illnesses. Vectors are created by resizing images.

They are then scaled to fit the training method [17]. The following step is to transform each image in the collection to an array. The image is used as a preprocessed input by MobileNetV2. The final level is coding. The tagged dataset is converted into a numerical label, which can then be understood and evaluated. Furthermore, random selection is used in the dataset to guarantee that the data is adequately disseminated.

D. Training and Testing

The training phase extracts properties from the dataset, while the testing phase assesses how well the appropriate model predicts. The dataset is divided into two sections. This is the time for training and testing. In K fold cross-validation, a single fold is utilized for testing and k-1 folds are used for training in a cyclical method. To avoid over fitting, cross-validation is performed. In this paper, we partition data using a five-fold cross-validation strategy, with four fold used for training and one-fold used for testing in each iteration.

E. Performance Measurements

Following the labeling of all pixels I_j in the input slice, P_{ij} as illustrated in equation (1) and (2). From vector f_l , $l = 1, 2, 3$, the classification function predicts the label l_p , that pinpoints the kind of tumor in a slice. The classification function determines the link between predicted label sizes, l , $P_{ij} == 1$, and the overall prediction, $P_{ij} > 0$. The projected label, l_p , will be the label with the largest capacity connection i.e. greater than the confidence threshold's minimum size relation, $\zeta_c \in [0, 1]$.

$$P_{ij} = \begin{cases} = 0, & \text{if (i,j) is healthy position} \\ = 1, & \text{if (i,j) is meningioma tumor} \\ = 2, & \text{if (i,j) is glioma tumor} \\ = 3, & \text{if (i,j) is pituitary tumor} \end{cases} \quad (1)$$

$$f_l = \begin{cases} \frac{P_{ij}==1}{P_{ij}>0} > \zeta_c \\ 0 \end{cases} \quad (2)$$

F. Image Classification Performance Metrics

Several metrics, including accuracy, precision, recall, F1-score, and AUC, were employed to evaluate performance of our scheme.

V. MACHINE LEARNING TECHNIQUES

When using traditional Machine Learning approaches, a preprocessing stage aimed at feature extraction is included in the segmentation pipeline [8]. The recovered attributes are then passed on to the classification or segmentation stage [7]. The ML inquiry would inquire whether or not the tumor is likely to be malignant (1=Yes, 0=No). Some important techniques to improve the performance of ML approaches are discussed below:

- 1) dimensionality reduction
- 2) feature selection
- 3) feature extraction

	0	1	2	3	4	5	6	7	8	9	...	150519	150520	150521	150522	150523
0	0.000000	0.000000	0.000000	0.000000	0.000000	0.000000	0.000000	0.000000	0.000000	0.000000	...	0.000000	0.000000	0.000000	0.000000	0.000000
1	0.000000	0.000000	0.000000	0.000000	0.000000	0.000000	0.000000	0.000000	0.000000	0.000000	...	0.000000	0.000000	0.000000	0.000000	0.000000
2	0.000000	0.000000	0.000000	0.000000	0.000000	0.000000	0.000000	0.000000	0.000000	0.000000	...	0.000000	0.000000	0.000000	0.000000	0.000000
3	0.000000	0.000000	0.000000	0.000000	0.000000	0.000000	0.000000	0.000000	0.000000	0.000000	...	0.000000	0.000000	0.000000	0.000000	0.000000
4	0.000000	0.000000	0.000000	0.000000	0.000000	0.000000	0.000000	0.000000	0.000000	0.000000	...	0.000000	0.000000	0.000000	0.000000	0.000000
...
248	0.140870	0.140870	0.140870	0.070387	0.070387	0.070387	0.062868	0.062868	0.062868	0.085950	...	0.078256	0.078256	0.078256	0.078256	0.078256
249	0.003922	0.003922	0.003922	0.003922	0.003922	0.003922	0.003922	0.003922	0.003922	0.003922	...	0.003922	0.003922	0.003922	0.003922	0.003922
250	0.143616	0.143616	0.143616	0.345293	0.345293	0.345293	0.301732	0.301732	0.301732	0.265334	...	0.272768	0.272768	0.272768	0.243786	0.243786
251	0.000000	0.000000	0.000000	0.000000	0.000000	0.000000	0.000000	0.000000	0.000000	0.000000	...	0.105882	0.105882	0.105882	0.108438	0.108438
252	0.119553	0.119553	0.119553	0.119553	0.119553	0.119553	0.119553	0.119553	0.119553	0.119553	...	0.080296	0.080296	0.080296	0.078648	0.078648

253 rows × 150529 columns

Fig. 1. Data Set of Brain Tumor

150524	150525	150526	150527	Target
0.000000	0.000000	0.000000	0.000000	0
0.000000	0.000000	0.000000	0.000000	0
0.000000	0.000000	0.000000	0.000000	0
0.000000	0.000000	0.000000	0.000000	0
0.000000	0.000000	0.000000	0.000000	0
...
0.078256	0.133088	0.133088	0.133088	1
0.003922	0.003922	0.003922	0.003922	1
0.243786	0.237173	0.237173	0.237173	1
0.108438	0.113270	0.113270	0.113270	1
0.078648	0.082783	0.082783	0.082783	1

Fig. 2. Segment of Fig. 1

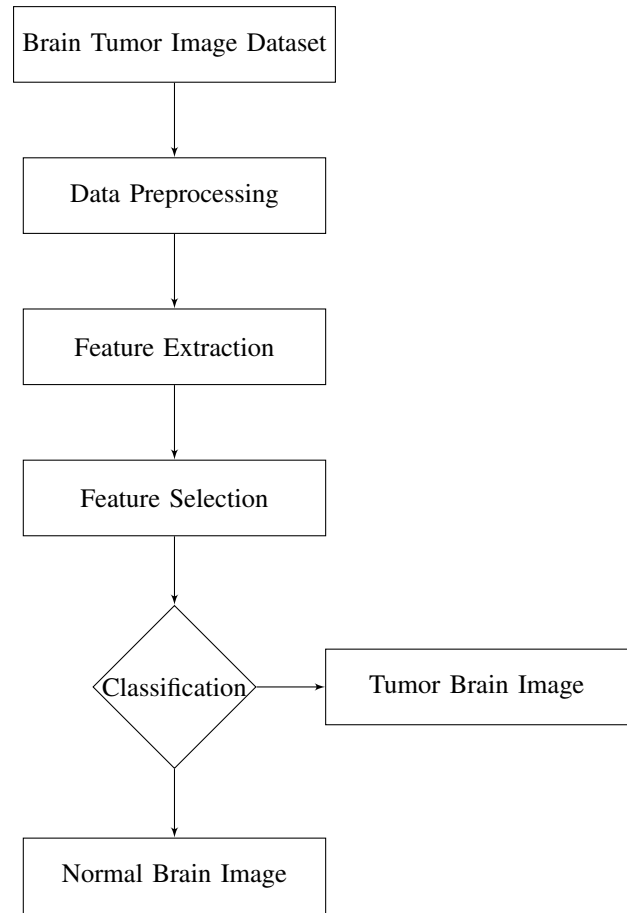


Fig. 3. Block Diagram

A. Support Vector Machine Algorithm

SVM or Support Vector Machine, may be employed for regression along with classification applications. SVMs offer much greater search accuracy than typical query refinement techniques after only 3 to 4 rounds of relevance feedback, according to simulated data. The SVM algorithm is frequently used in clinical and other disciplines. We will be utilizing the brain tumor dataset to develop our SVM method.

The F1-score for healthy and brain tumor categorization is 86% and 92%, respectively in Fig. 4. We can see from the

output of Fig. 4 that there were some inaccurate predictions; thus, if we want to determine the number of correct and incorrect predictions, we must utilize the confusion matrix. The confusion matrix is shown in the output graphic in Fig. 5, with 4+1=5 wrong guesses and 16+30=46 right predictions.

	precision	recall	f1-score	support
0	0.94	0.80	0.86	20
1	0.88	0.97	0.92	31
accuracy			0.90	51
macro avg	0.91	0.88	0.89	51
weighted avg	0.91	0.90	0.90	51

Fig. 4. Classification Metrics of SVM

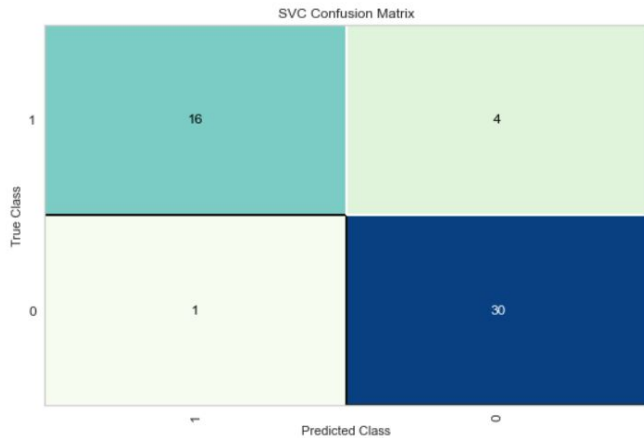


Fig. 5. Confusion Matrix for SVM Classifier

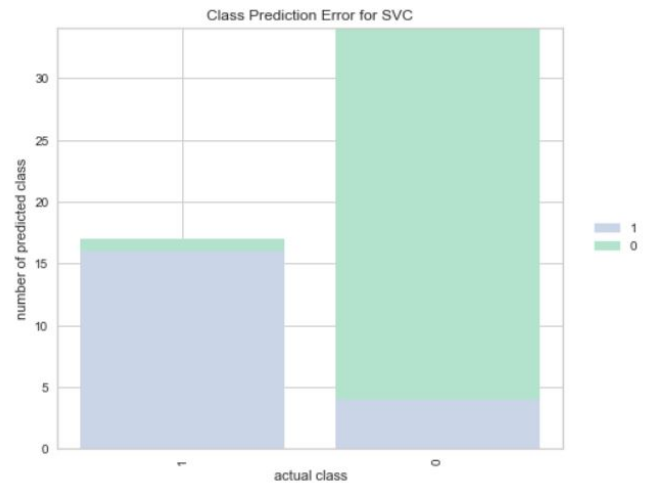


Fig. 7. Visualizer for SVM Classifier

	precision	recall	f1-score	support
0	0.76	0.65	0.70	20
1	0.79	0.87	0.83	31
accuracy			0.78	51
macro avg	0.78	0.76	0.77	51
weighted avg	0.78	0.78	0.78	51

Fig. 8. Classification Metrics for DTREE Classifier

The graphical depiction of the results in terms of ROC and micro-average ROC curve is shown in Fig. 6. We will draw a graph for the SVM classifier in Fig. 7 to illustrate the training set outcome. The classifier will determine whether a brain tumor is malignant or benign.

B. Decision Tree

Decision Tree (DTree) is a Supervised learning approach and tree structured that can be utilized to solve classification problems. Here the internal nodes represents attribute, branch represent rules and leaf node specifies conclusion. It is a

graphical depiction of solutions to a problem depending on specific criteria.

The F1-score for healthy and brain tumour categorization is 70% and 83%, respectively in Fig. 8. We can see from the output of Fig. 8 that there were some inaccurate predictions; thus, if we want to determine the number of correct and incorrect predictions, we must utilize the confusion matrix. The confusion matrix is shown in the output Fig. 9, with 4+7=11 inaccurate guesses and 13+27=40 right predictions.

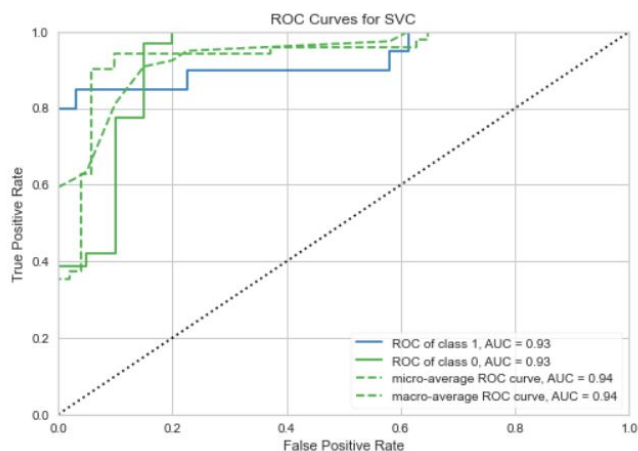


Fig. 6. ROC for SVM Classifier

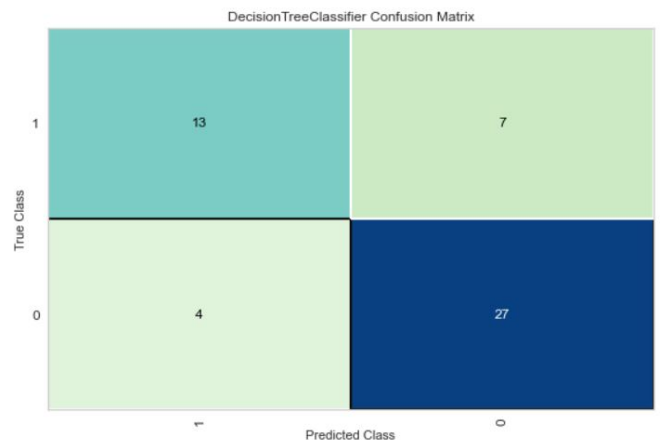


Fig. 9. Confusion Matrix for DTREE Classifier

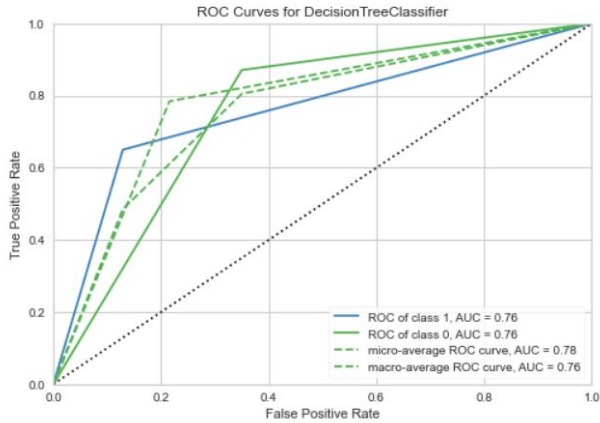


Fig. 10. ROC for DTREE Classifier

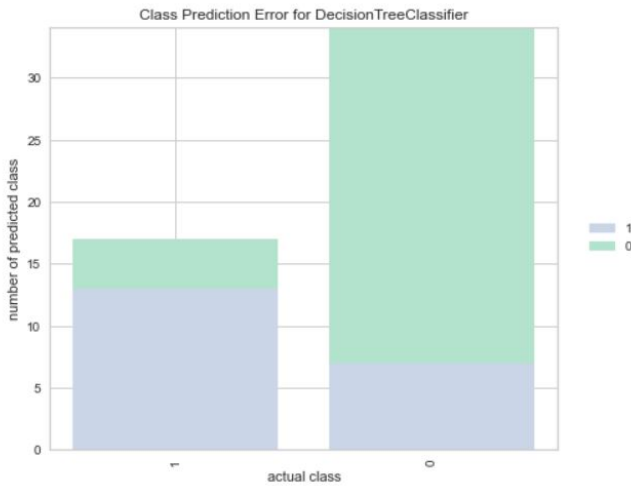


Fig. 11. Visualizer for DTREE Classifier

The graphical depiction of the results in terms of ROC and micro-average ROC curve is shown in Fig. 10. The above output is completely different from the rest classification models. We will plot a graph for the decision tree classifier in Fig. 11 to view the training set outcome. The classifier will determine whether a brain tumor is malignant or benign.

C. Gaussian Naive Bayes

Gaussian Naive Bayes is the name given to the generalization of naive Bayes. The normal distribution (Gaussian distribution) is simpler to use as it can estimate mean and standard deviation very quickly from the training data. A Gaussian distribution is assumed if the input variables are real-valued. This may need the removal of outliers.

The F1-score for normal and brain tumor categorization is 81% and 87%, respectively which is represented in Fig. 12. The confusion matrix is shown in the output Fig. 13, with 3+5=8 inaccurate guesses and 17+26=43 right predictions.

The graphical depiction of the results in terms of ROC and micro-average ROC curve is shown in Fig. 14. We will draw

	precision	recall	f1-score	support
0	0.77	0.85	0.81	20
1	0.90	0.84	0.87	31
accuracy			0.84	51
macro avg	0.83	0.84	0.84	51
weighted avg	0.85	0.84	0.84	51

Fig. 12. Classification Metrics for Gaussian NB Classifier

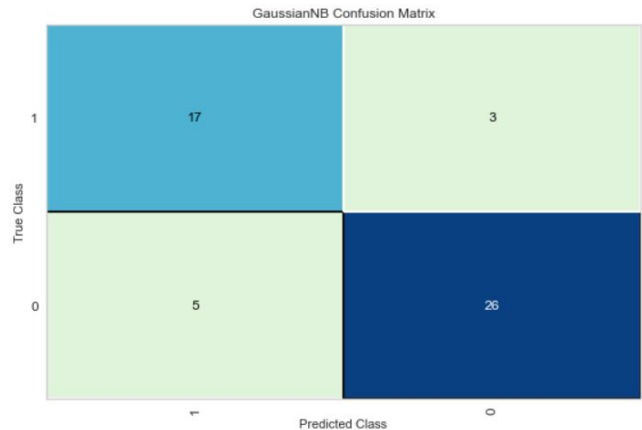


Fig. 13. Confusion Matrix for Gaussian NB Classifier

a graph in Fig. 15 for the Gaussian NB classifier to show the training set outcome. The classifier will determine whether a brain tumor is malignant or benign.

D. Random Forest

Random forest chooses observations at random, creates a decision tree, and uses the average result. Random Forest classifiers can handle both categorized as well as continuous variables in an effective manner. It outperforms other algorithms in categorization tasks. It is capable of handling binary,

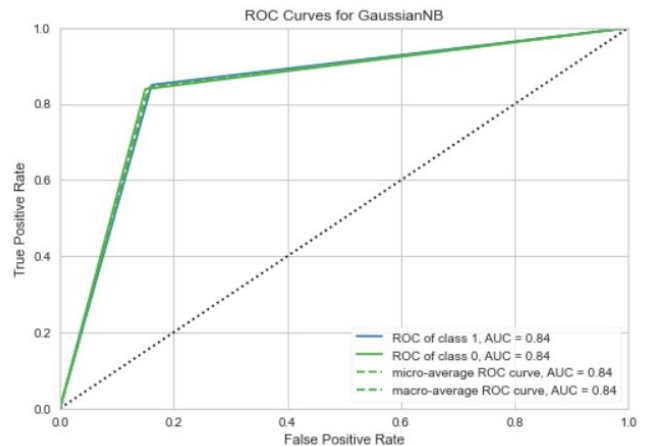


Fig. 14. ROC for Gaussian NB Classifier

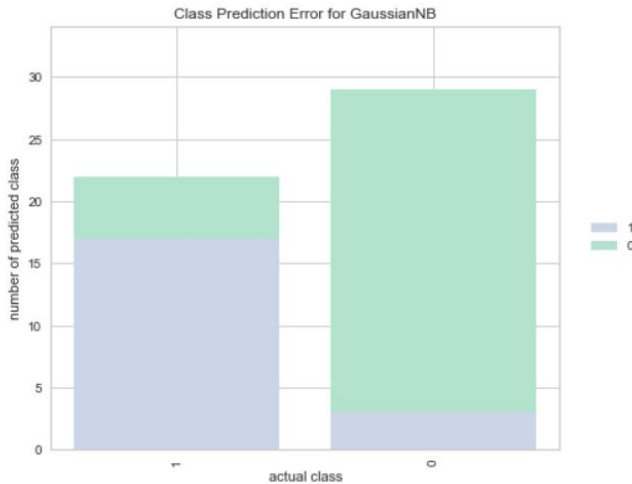


Fig. 15. Visualizer for Gaussian NB Classifier

	precision	recall	f1-score	support
0	1.00	0.85	0.92	20
1	0.91	1.00	0.95	31
accuracy			0.94	51
macro avg	0.96	0.93	0.94	51
weighted avg	0.95	0.94	0.94	51

Fig. 16. Classification Metrics for Random Forest Classifier

continuous, and categorical data.

The F1-score for healthy and brain tumor categorization is 92% and 95%, respectively in Fig. 16. The confusion matrix is constructed in the output image Fig. 17 to identify the accurate and wrong guesses, which contains 3+0=3 erroneous predictions and 17+31=48 correct predictions.

The graphical depiction of the results in terms of ROC and micro-average ROC curve is shown in Fig. 18. The above output is completely different from the rest classification

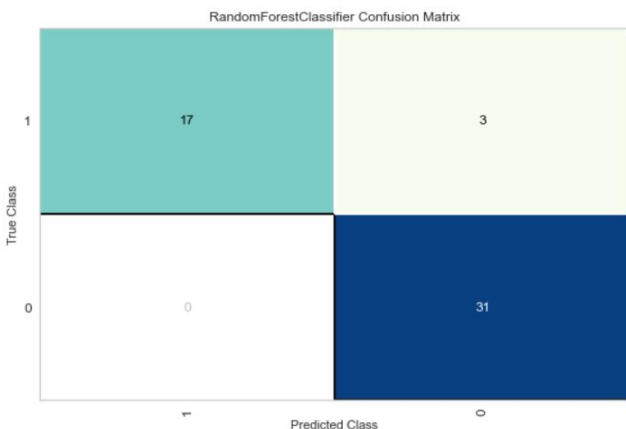


Fig. 17. Confusion Matrix for Random Forest Classifier

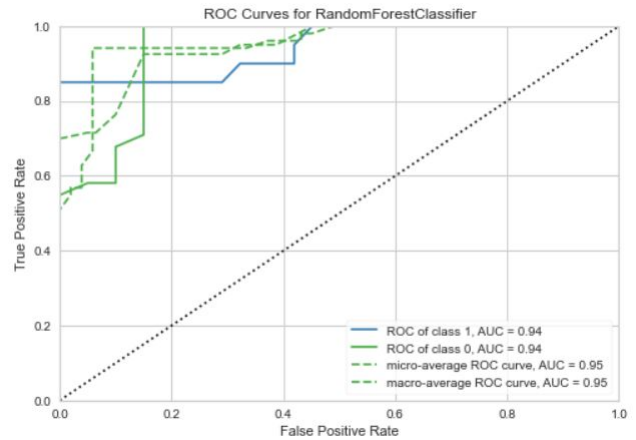


Fig. 18. ROC for Random Forest Classifier

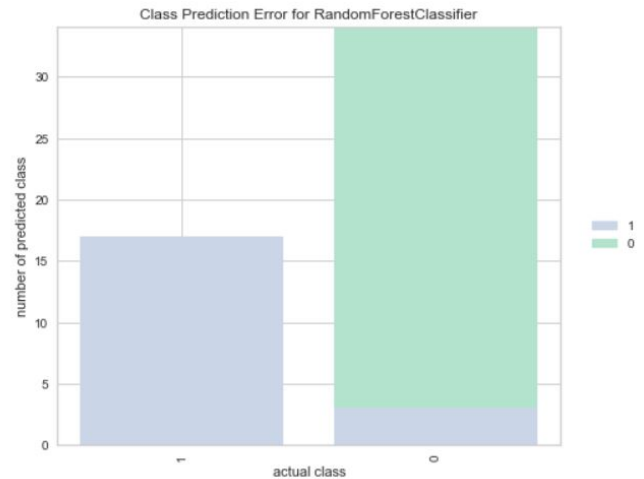


Fig. 19. Visualizer for Random Forest Classifier

models. We will create a graph for the Random Forest classifier to view the training set results in Fig. 19. The classifier will determine whether a brain tumor is malignant or benign.

E. Multinomial Naive Bayes Classifier

Multinomial Naive Bayes can be treated as a probabilistic process and is extensively utilized for categorical training set. It helps in obtaining highest likelihood. Normally, the multinomial distribution requires integer feature counts.

The F1-score for normal and brain tumor categorization is

	0	0.78	0.70	0.74	20
1	0.82	0.87	0.84		31
accuracy				0.80	51
macro avg	0.80	0.79	0.79		51
weighted avg	0.80	0.80	0.80		51

Fig. 20. Classification Metrics for Multinomial NB Classifier

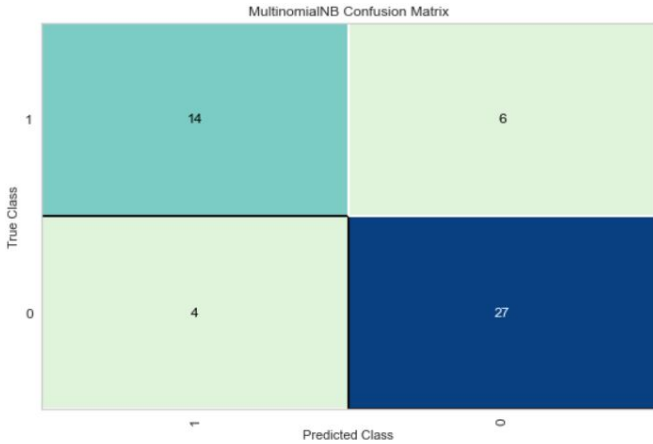


Fig. 21. Confusion Matrix for Multinomial NB Classifier

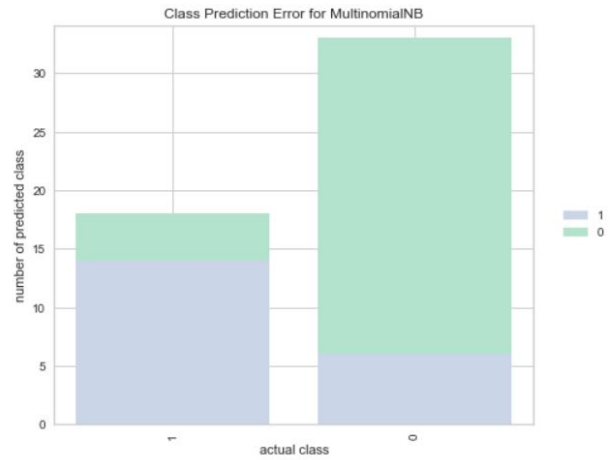


Fig. 23. Visualizer for Multinomial NB Classifier

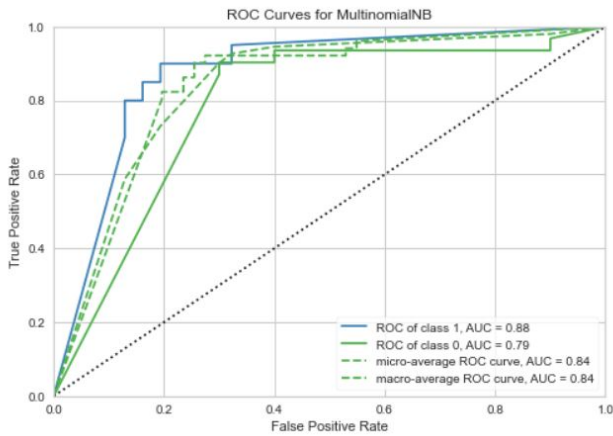


Fig. 22. ROC for Multinomial NB Classifier

	precision	recall	f1-score	support
0	1.00	0.85	0.92	20
1	0.91	1.00	0.95	31
accuracy			0.94	51
macro avg	0.96	0.93	0.94	51
weighted avg	0.95	0.94	0.94	51

Fig. 24. Classification Metrics for Extreme Gradient Boost Classifier

74% and 84%, respectively in Fig. 20. In Fig. 21, a confusion matrix is used to determine the correct and incorrect guesses, with $6+4=10$ incorrect forecasts and $14+27=41$ accurate predictions.

The graphical depiction of the results in terms of ROC and micro-average ROC curve is shown in Fig. 22. The above output is completely different from the rest classification models. We will draw a graph of Fig. 23 for the Multinomial NB classifier to show the training set outcome. The classifier will determine whether a brain tumor is malignant or benign.

F. Extreme Gradient Boost (XGB) Classifier

This classifier is treated as a boosted classifier for tabular as well as structured training samples. At the same time, it has the characteristic to handle complex and huge databases. It is a technique for ensemble modeling.

The F1-score for healthy and brain tumor categorization is 92% and 95%, respectively in Fig. 24. In Fig. 25, a confusion matrix is used to determine the correct and incorrect guesses, with $3+0=3$ erroneous forecasts and $17+31=48$ accurate predictions.

The graphical depiction of the results in terms of ROC and micro-average ROC curve is shown in Fig. 26. To display the training set outcome, we will create a graph for the XGB classifier in Fig. 27. The classifier will determine whether the brain tumor is malignant or benign. XGBoost is more than 10 times quicker.

G. Stochastic Gradient Descent (SGD) Classifier

A gradient is the slope of a function. It assesses the degree to which one variable changes in response to changes in

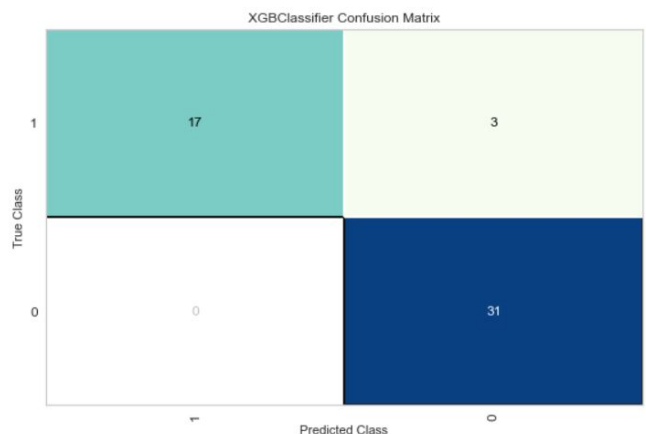


Fig. 25. Confusion Matrix for XGB Classifier

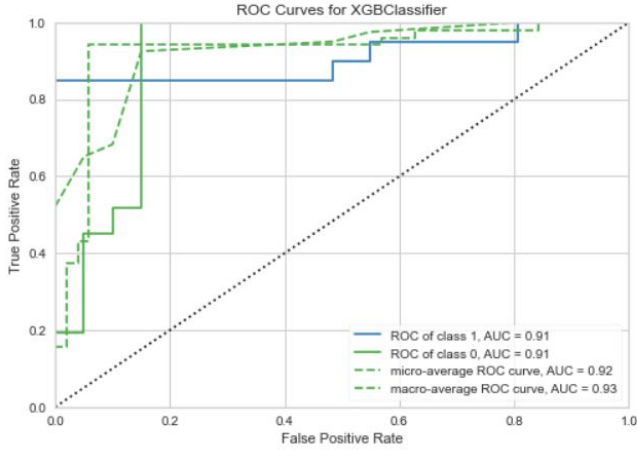


Fig. 26. ROC for XGB Classifier

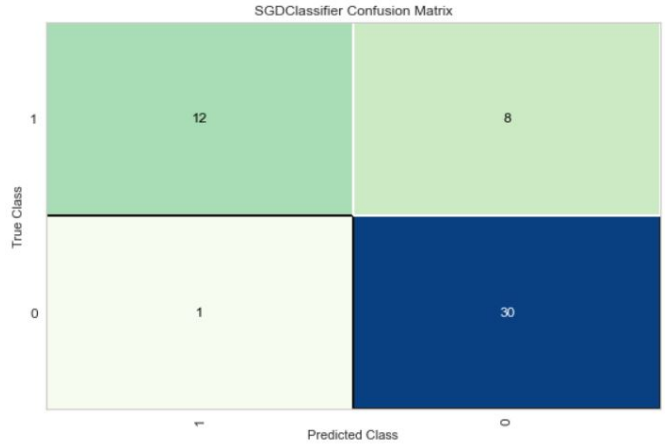


Fig. 29. Confusion Matrix for SGD Classifier

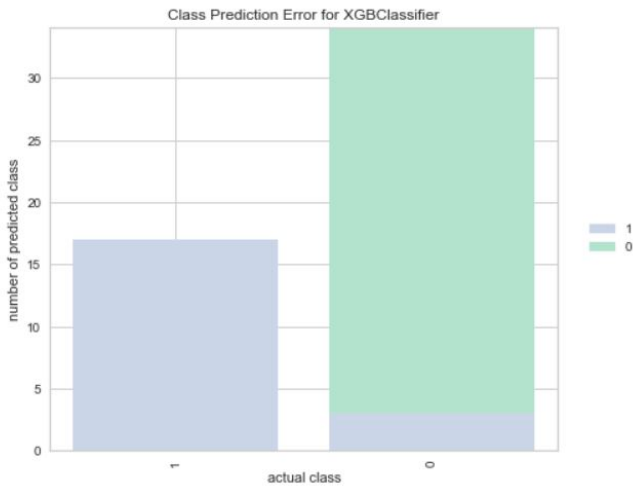


Fig. 27. Visualizer for XGB Classifier

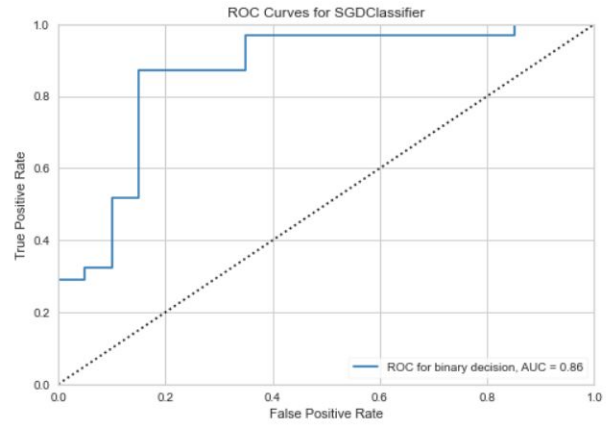


Fig. 30. ROC for SGD Classifier

another one. The steeper the slope, the higher the gradient value. It computes gradient using a single training sample. It is quicker and less computationally costly than batch gradient descent.

The F1-score for healthy and brain tumor categorization is 73% and 87%, respectively in Fig. 28. In the graph of Fig. 29, a confusion matrix is used to determine the correct and incorrect guesses, with $8+1=9$ incorrect forecasts and $12+30=42$ accurate predictions.

	precision	recall	f1-score	support
0	0.92	0.60	0.73	20
1	0.79	0.97	0.87	31
accuracy			0.82	51
macro avg	0.86	0.78	0.80	51
weighted avg	0.84	0.82	0.81	51

Fig. 28. Classification Metrics for SGD Classifier

The graphical depiction of the results in terms of ROC and micro-average ROC curve is shown in Fig. 30. The above output is completely different from the rest classification models. We will plot a graph for the SGD classifier in Fig. 31 to visualize the training set outcome. The classifier will determine whether a brain tumor is malignant or benign.

H. Bagging Classifier

Bagging lowers over fitting (variance) by averaging or voting; nevertheless, this increases bias, which is offset by the decrease in variance. Bagging builds n classification trees from the training data using bootstrap sampling and then combines their predictions to get a final meta-prediction. Bagging and decision trees can be combined and used to eliminate overfitting.

The F1-score for healthy and brain tumor categorization is 90% and 94%, respectively in Fig. 32. In the graphic of Fig. 33, a confusion matrix is used to calculate the correct and incorrect guesses, with $2+2=4$ incorrect predictions and $18+29=47$ accurate predictions.

The graphical depiction of the results in terms of ROC and micro-average ROC curve is shown in Fig. 34. The above

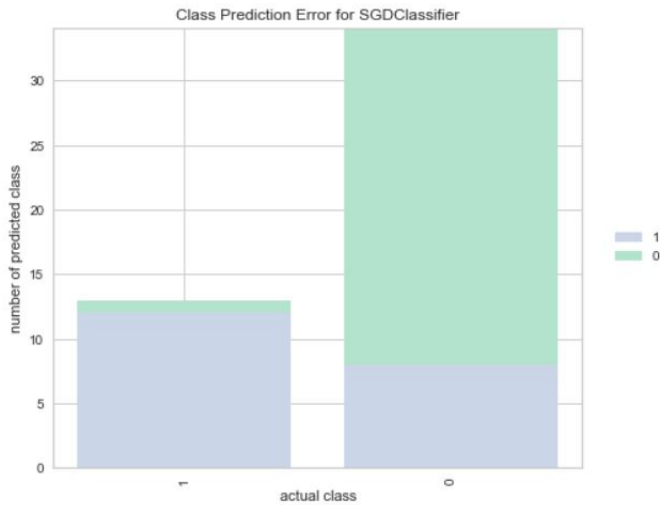


Fig. 31. Visualizer for SGD Classifier

	precision	recall	f1-score	support
0	0.90	0.90	0.90	20
1	0.94	0.94	0.94	31
accuracy			0.92	51
macro avg	0.92	0.92	0.92	51
weighted avg	0.92	0.92	0.92	51

Fig. 32. Classification Metrics for BAG Classifier

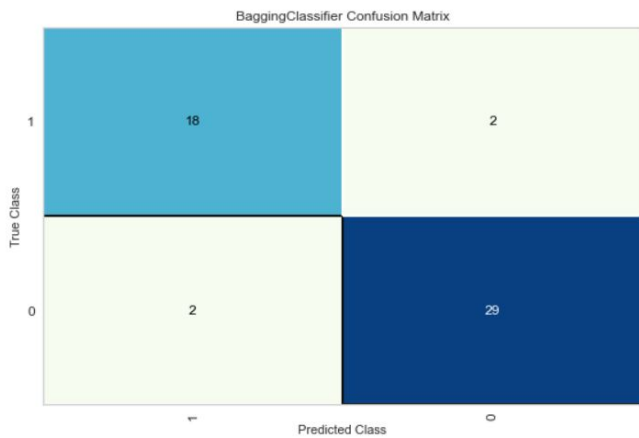


Fig. 33. Confusion Matrix for BAG Classifier

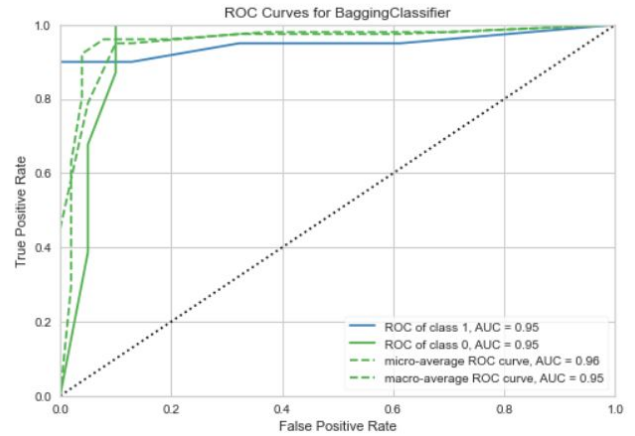


Fig. 34. ROC for BAG Classifier

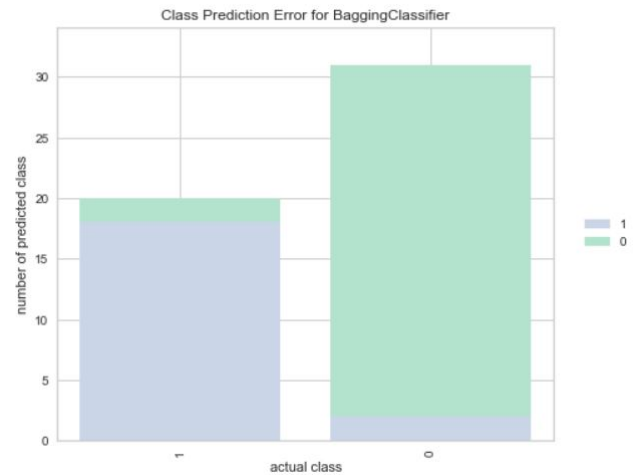


Fig. 35. Visualizer for BAG Classifier

output is completely different from the rest classification models. We will plot a graph for the BAG classifier in Fig. 35 to visualize the training set outcome. The classifier will determine whether a brain tumor is malignant or benign.

I. LGBM Classifiers

Light GBM can handle enormous quantities of data while consuming minimal memory. It emphasises result precision. LGBM also supports GPU learning, therefore scientists are

	precision	recall	f1-score	support
0	0.94	0.80	0.86	20
1	0.88	0.97	0.92	31
accuracy			0.90	51
macro avg	0.91	0.88	0.89	51
weighted avg	0.91	0.90	0.90	51

Fig. 36. Classification Metrics for LGBM Classifier

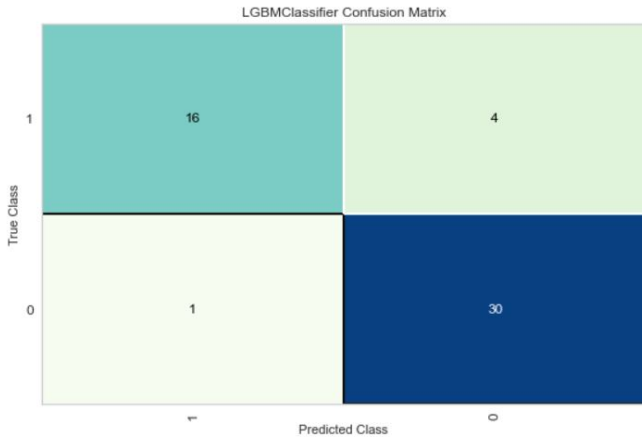


Fig. 37. Confusion Matrix for LGBM Classifier

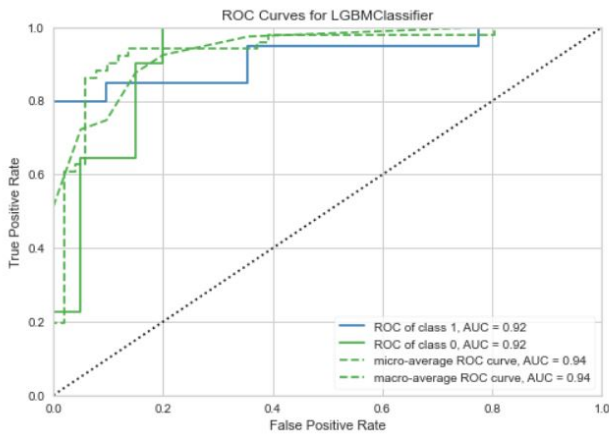


Fig. 38. ROC for LGBM Classifier

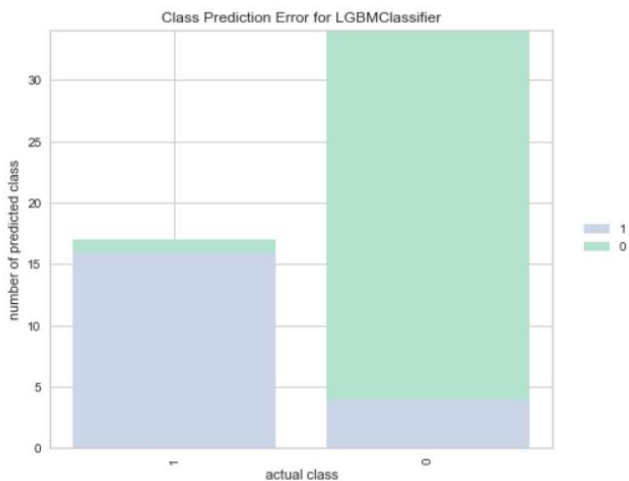


Fig. 39. Visualizer for LGBM Classifier

	model	best_score	best_params
0	svm	0.747805	{'C': 30, 'kernel': 'rbf'}
1	random_forest	0.772561	{'n_estimators': 10}
2	logi_reg	0.757805	{'C': 1}
3	gNB	0.757805	{'var_smoothing': 0.02310129700083159}
4	mNB	0.688293	{'alpha': 0.9, 'fit_prior': True}
5	bGC	0.816829	{'max_features': 30, 'n_estimators': 70}
6	dDC	0.757195	{'criterion': 'gini', 'max_depth': 5, 'min_sam...
7	Xgb	0.801829	{'colsample_bytree': 0.8, 'gamma': 0, 'learnin...
8	SGD	0.743293	{'loss': 'hinge', 'penalty': 'l2'}

Fig. 40. Comparison of different Techniques of Machine Learning for the Prediction of Brain Cancer in GridSearchCV

	model	best_score	best_params
0	svm	0.747805	{'kernel': 'rbf', 'C': 30}
1	random_forest	0.787073	{'n_estimators': 30}
2	logi_reg	0.757805	{'C': 1}
3	gNB	0.757805	{'var_smoothing': 0.02310129700083159}
4	mNB	0.688293	{'fit_prior': True, 'alpha': 0.9}
5	bGC	0.821829	{'n_estimators': 70, 'max_features': 10}
6	dDC	0.757195	{'min_samples_leaf': 5, 'max_depth': 5, 'crite...
7	Xgb	0.801829	{'subsample': 0.8, 'seed': 27, 'scale_pos_weig...
8	SGD	0.753049	{'penalty': 'elasticnet', 'loss': 'log'}

Fig. 41. Comparison of different Techniques of Machine Learning for the Prediction of Brain Cancer in RandomizedSearchCV

utilizing it to build research applications. LGBM should not be used to small datasets.

The F1-score for healthy and brain tumor classification is 86% and 92%, respectively in Fig. 36. A confusion matrix is used in the graph of Fig. 37 to calculate the correct and incorrect guesses, with 4+1=5 incorrect predictions and 16+30=46 accurate predictions.

The graphical depiction of the results in terms of ROC and micro-average ROC curve is shown in Fig. 38. The above output is completely different from the rest classification models. To illustrate the training set outcome, we shall draw a graph for the LGBM classifier in Fig. 39. The classifier will evaluate whether a brain tumor is benign or malignant.

VI. EXPERIMENTAL ANALYSIS AND RESULT

We compared all the techniques used for the prediction of brain cancer by different parameters in grid search CV (Fig. 40) and randomized search CV (Fig. 41), respectively. The proposed method was implemented in Python by using 5-fold cross validation techniques. Our experimental result proves that all the nine classifier are providing good results with respect to different parameters values. However, for both GridSearchCV and RandomizedSearchCV bagging classifier is giving best results.

VII. CONCLUSION

Our article employs data augmentation approach prior to classification to avoid overfitting. We surveyed some popular state-of-the-art machine learning approaches to reach at a conclusion. Our work is experimented on T1-weighted contrast-enhanced MRI images. However, this study reveals the importance of supervised learning approaches on devising CAD systems to reduce the burden of radiologists. A future exploration can be extended in collecting some larger brain MR images to generalize the classifier systems.

REFERENCES

- [1] Hanahan, D., and Weinberg, R. A. (2011). Hallmarks of cancer: the next generation. *cell*, 144(5), 646-674.
- [2] Işın, A., Direkoğlu, C., and Şah, M. (2016). Review of MRI-based brain tumor image segmentation using deep learning methods. *Procedia Computer Science*, 102, 317-324.
- [3] Sachdeva, J., Kumar, V., Gupta, I., Khandelwal, N., & Ahuja, C. K. (2016). A package-SFERCB-"Segmentation, feature extraction, reduction and classification analysis by both SVM and ANN for brain tumors". *Applied soft computing*, 47, 151-167.
- [4] Kaur, N., & kaur Panag, N. (2016). A Review on Brain tumour segmentation.
- [5] Iftekharruddin, K. M., Zheng, J., Islam, M. A., & Ogg, R. J. (2009). Fractal-based brain tumor detection in multimodal MRI. *Applied Mathematics and Computation*, 207(1), 23-41.
- [6] Havaei, M., Jodoin, P. M., & Larochelle, H. (2014, August). Efficient interactive brain tumor segmentation as within-brain kNN classification. In *2014 22nd international conference on pattern recognition* (pp. 556-561). IEEE.
- [7] Bishop, C. M., & Nasrabadi, N. M. (2006). *Pattern recognition and machine learning* (Vol. 4, No. 4, p. 738). New York: springer.
- [8] Chaddad, A., & Tanougast, C. (2016). Quantitative evaluation of robust skull stripping and tumor detection applied to axial MR images. *Brain informatics*, 3(1), 53-61.
- [9] Mohsen, H., El-Dahshan, E. S. A., El-Horbaty, E. S. M., & Salem, A. B. M. (2018). Classification using deep learning neural networks for brain tumors. *Future Computing and Informatics Journal*, 3(1), 68-71.
- [10] Abiwinanda, N.; Hanif, M.; Hesaputra, S.T.; Handayani, A.; Mengko, T.R. Brain tumor classification using convolutional neural network. In *Proceedings of the World Congress on Medical Physics and Biomedical Engineering*, Prague, Czech Republic, 3-8 June 2018; Springer: Singapore, 2019; pp. 183-189.
- [11] Pashaei, A., Sajedi, H., & Jazayeri, N. (2018, October). Brain tumor classification via convolutional neural network and extreme learning machines. In *2018 8th International conference on computer and knowledge engineering (ICCKE)* (pp. 314-319). IEEE.
- [12] Sultan, H. H., Salem, N. M., & Al-Atabany, W. (2019). Multi-classification of brain tumor images using deep neural network. *IEEE Access*, 7, 69215-69225.
- [13] Anaraki, A. K., Ayati, M., & Kazemi, F. (2019). Magnetic resonance imaging-based brain tumor grades classification and grading via convolutional neural networks and genetic algorithms. *biocybernetics and biomedical engineering*, 39(1), 63-74.
- [14] Manikis, G. C., Emmanouilidou, D., Sakkalis, V., Graf, N., & Marias, K. (2011, November). A fully automated image analysis framework for quantitative assessment of temporal tumor changes. In *2011 E-Health and Bioengineering Conference (EHB)* (pp. 1-6). IEEE.
- [15] Roy, S., Nag, S., Maitra, I. K., & Bandyopadhyay, S. K. (2013). A review on automated brain tumor detection and segmentation from MRI of brain. *arXiv preprint arXiv:1312.6150*.
- [16] Wang, T., Manohar, N., Lei, Y., Dhabaan, A., Shu, H. K., Liu, T., ... & Yang, X. (2019). MRI-based treatment planning for brain stereotactic radiosurgery: dosimetric validation of a learning-based pseudo-CT generation method. *Medical Dosimetry*, 44(3), 199-204.
- [17] Kotte, S., Pullakura, R. K., & Injeti, S. K. (2018). Optimal multilevel thresholding selection for brain MRI image segmentation based on adaptive wind driven optimization. *Measurement*, 130, 340-361.